Multifunctional sol-gel derived thin film based on nanocrystaline hydroxyapatite powders

Multifunctional sol-gel derived thin film based on nanocrystaline hydroxyapatite powders

A.A. El hadad [1], **V. Barranco** [2], **A. Jiménez-Morales** [3], **E. Peon** [4], **J.C. Galván** [1]

[1]Centro Nacional de Investigaciones Metalúrgicas (CSIC), Madrid, Spain. [2]Instituto de Ciencia de Materiales de Madrid (CSIC), Madrid, Spain. [3]Universidad Carlos III de Madrid. Departamento de Ciencia e Ingeniería de Materiales e Ingeniería Química. (Madrid), Spain. [4]Centro de Biomateriales, Universidad de La Habana, Havana, Cuba

E-mails: amirelhadad@cenim.csic.es, jcgalvan@cenim.csic.es

Abstract. The aim of this work was to prepare bioactive hydroxyapatite coatings by sol-gel method and to study the effect of thermal treatment temperature upon the bioactivity and corrosion protection of these coatings on Ti6Al4V alloy. The application of (DTA/TGA) and (XRD) has provided valuable information about the phase transformation, mass loss, identification of the phases developed, crystallite size and degree of crystallinity. (SEM/EDX) has been applied to study the surface morphology of coated samples before and after immersion in simulated body fluid (SBF) to detect the biomimetic precipitation of the bone-like apatite. The obtained results show that all the prepared samples are ceramic nanocrystalline with crystal structure and composition like hydroxyapatite, with little deviations from that present in the human bone. The bioactivity of the studied samples is found to be closely related to the thermal treatments applied. That is, the bioactivity decreases as the temperature of the thermal treatment increase. Coatings from such prepared hydroxyapatite sol have been accomplished by dip-coating technique on non-toxic Ti6Al4V alloy for biomedical applications. The corrosion behaviour of the resulting hydroxyapatite coatings in a (SBF) has been studied by electrochemical impedance spectroscopy (EIS). The hydroxyapatite coated Ti6Al4V alloy displayed excellent bioactivity when soaked in the (SBF) and acceptable corrosion protection behaviour.

1. Introduction

The bone tissue is considered as a natural composite, composed of two constituents organic and inorganic solid, the inorganic solid is carbonated hydroxyapatite (CHA) while the organic one is collagen. The hydroxyapatite (HA) which has the formula $Ca_{10}(PO_4)_6(OH)_2$, amounts to 65% of the total bone mass, with the remaining mass formed by organic matter "mostly collagen" and water[1]. The collagen molecules are bonded together forming fibrils, which bound together to form fibers. Between these fibers there are small interstitial empty spaces, where apatite nanocrystals are deposited. For this reason, the most used calcium phosphate in implant fabrication is HA, a biological active material with different forms, particles, films, coatings, fibers which has extensive biomedical applications [2]. Nano-sized HA powders have a high specific surface area and therefore exhibit enhanced activity toward chemical and biological interactions in the human body. HA has been known to form *in vitro* and *in vivo* a bioactive bone-like apatite layer spontaneously on its surfaces. The formed apatite layer act as interface between the implant and tissue, facilitate the formation of chemical and biological bond with the osseous tissue. Therefore, the essential prerequisite for a biomaterial to bond

directly to living bone is the formation of an apatite layer on its surface when implanted in the body. As this layer is formed, the protein absorption onto the surface of such layer will trigger the osteoblasts, "new bone forming cells", to differentiate and reproduce, leading the formation of new bone tissue.

The HA can be synthesized by many methods [3,4]. Among all of them, the sol-gel process is the most used technique for production of HA because it offers many advantages over other traditional methods. It allows the production of ultra fine and pure ceramic powders with relatively low cost, low synthesis temperature, ability to coat porous and complex surfaces with high control of composition and microstructure of the obtained film [5-7]. The HA synthesized by sol-gel will form strong chemical bonds with bone *in vivo*, all of these mentioned properties place the HA into a class of biomaterials known as bioactive materials. Unfortunately brittleness limits its usage for load bearing applications. For that it can only be used as bone fillers and bone graft substitutes in orthopedics[8]. The only exception where HA is applied in dynamically loaded situations is the use of HA as a coating material.

In the present study, HA was synthesized by adopting a sol–gel approach. The resultant HA was characterized using DTA, TGA, XRD and SEM/EDX techniques. Sol–gel-derived HA coatings on Ti6Al4V substrate were evaluated via electrochemical studies involving impedance measurements in Kokubo's simulated body fluid (SBF) solution.

2. Experimental
2-1. Preparation of Hydroxyapatite Powders.
The prepared HA sol-gel was obtained by hydrolysis and condensation of two precursors. Triethyl phosphite, $(C_2H_5O)_3P$ (Fluka) and calcium nitrate tetrahydrate, $Ca(NO_3)_2 \cdot 4H_2O$ (Panreac) were employed as phosphorus and calcium precursors respectively. In brief, 0.03mol of triethyl phosphite was first diluted in ethanol and hydrolyzed for 24 h with a fixed amount of distilled water in a parafilm-sealed glass container under vigorous stirring.

A stoichiometric amount, 0.05 moles, of $Ca(NO_3)_2 \cdot 4H_2O$ is dissolved first in 25 ml of anhydrous ethanol then added dropwise into the hydrolyzed phosphite sol. The mixed sol solution was then continuously agitated for additional 30 min and kept static (aging) at 45^oC. The pH value was adjusted to be 7.5; the sol was aged static at 60^oC for 16 h. The solvents were then driven off resulting in a viscous liquid. Further drying at 80^oC was done to obtain the prepared material in a powder form. The obtained powder was placed in a steel die, and pressed to 7 GPa to produce 12.9 mm diameter pellets which were was sintered at various temperatures (600, 800, and 1200^oC).

2-2. Preparation of HA Coatings on Ti6Al4V Substrates
Ti6Al4V disks of 2 cm of diameter and 0.4 cm of thickness were polished using different silicon carbide grit up to 1200 grade. The substrates were ultrasonically degreased with acetone for 10 min and washed with distilled water. Finally, the substrates were dried at 200^oC for 1 hour in an air oven to form a titanium oxide surface. These substrates were dip coated with the HA sol solution, with a dipping and withdraw speed of 12 cm/min. The sol-coated substrates were then immediately transferred into an air oven and held at 80^oC for 30 min. To increase the thickness of the coating, the above process was repeated for three times and finally it was sintered at various temperatures (600, 800^oC).

2.3 Characterization of HA Powder Samples

2.3.1 Thermal Behaviour (DTA/TGA)

The thermal behavior and mass loss of the powder was carried out using (**SETARAM DTA-TG** Setsys Evolution -1750), with α-Al_2O_3 powders as a reference material. HA powder samples with a weight of about 50 mg were analyzed. The samples and the reference material were heated in air from ambient temperature to 1300°C in argon at a heating rate of 20°C/min.

2.3.2 X-ray Diffractometer Analysis (XRD)

X-ray diffraction patterns have been recorded using a Siemens diffractometer D5000 equipped with scanning rate 0.1° in the 2θ ranging from 10° to 100° step time 1 sec. The prepared HA powder samples (S1 "as-prepared", S6 "treated at 600°C", S8 "treated at 800°C" and S12 "treated at 1200°C") were examined with a high-resolution X-ray powder diffractometer using monochromatic Cu Kα radiation (λ= 0.15406 nm). The results have been used to notice the change of developing phases, crystal structure of HA and degree of crystallinity, with the variation of heat treatment temperatures.

2.4. Evaluation of Bioactivity and Corrosion Protection

2.4.1 Immersion Tests of HA-Coatings/Ti6Al4V System in SBF

The *in vitro* bioactivity of the prepared HA-coatings/Ti6Al4V samples was tested by soaking in Kokubo's simulated body fluid (SBF). The pH of the SBF solution was buffered at 7.4. The specimens were immersed in separate plastic containers then incubated for 15 days at 37.5°C. After 15 days the specimens were removed from the solution, rinsed with distilled water and left to dry at room temperature.

2.4.2 Corrosion Behaviour

The corrosion behaviour of the HA-coatings/Ti6Al4V system was evaluated by applying electrochemical impedance spectroscopy measurements (EIS). For this purpose a potentiostat/galvanostat AutoLab EcoChemie PGSTAT30 (Eco Chemie, Utrecht, The Netherlands) equipped with a FRA2 frequency response analyzer module was used. A three electrode setup was applied. The working electrode was the investigated sample with an area of 2.14 cm^2. The reference and the counter-electrode were a saturated calomel electrode (SCE) and a large size graphite sheet, respectively. The electrochemical cell was filled with Kokubo's solution. The EIS measurements were made at the open circuit potential (OCP). Logarithmic frequency scans were carried out by applying sinusoidal wave perturbations of ±10mV in amplitude, in the range of 10^5-10^{-3}Hz. Five impedance sampling points were registered per frequency decade. The impedance data were analysed by using the 'EQUIVCRT' program developed by Boukamp (AC-Immittance Data Analysis System, Version 4.51, University of Twente, The Netherlands, 1993). The electrical resistance values were obtained by applying the fitting routines of the ZView® software version 3.1c (Scribner Associates Inc, Southern Pines, NC, USA).

2.4.3 Scanning Electron Microscopy (SEM/EDX)

The surface morphology of selected specimens, before and after immersion in SBF, was carried out by scanning electron microscopy (SEM) with a field emission gun (FEG) coupled with an energy dispersive X-ray (EDX) system (Oxford Inca microanalysis system and a windowless detector) for chemical analysis. The samples were examined in a JEOL-6500F microscope at 15 kV acceleration voltages. The samples were coated with ultra thin carbon conductive layer to avoid the charging due to the non conductive nature of the studied samples.

3. Results and discussion

Differential Thermal Analysis (DTA) and thermogravimetry (TG) diagrams of the obtained powders are given in Figure 1. The DTA was employed to determine the temperature at which the as-prepared powder, amorphous calcium phosphate (ACP), transforms to crystalline HA.

In the DTA curve of dry gel (powder), the first endothermic peak appeared at 38.8°C which was due to the evaporation of the absorbed water (residual moisture evaporation)[9]. The two endothermic peaks which appeared at 123.3°C and 443.2°C were attributed to elimination of crystalline water in un-reacted calcium nitrate tetra hydrate $Ca(NO_3)_2 4H_2O$ and removal of NO_3^- groups, as well as, to the condensation "dehydration" of hydrogen phosphate ions (HPO_4^{2-}) to form amorphous pyrophosphates ($P_2O_7^{4-}$) which is a component of amorphous calcium phosphates that forms during processing of HA synthesis[10-12]. The endothermic peak at 532.5°C is representative of the endothermic reaction indicating the crystallization of HA. The last endothermic peak observed at 1197.6°C may be attributed to the decomposition of the HA.
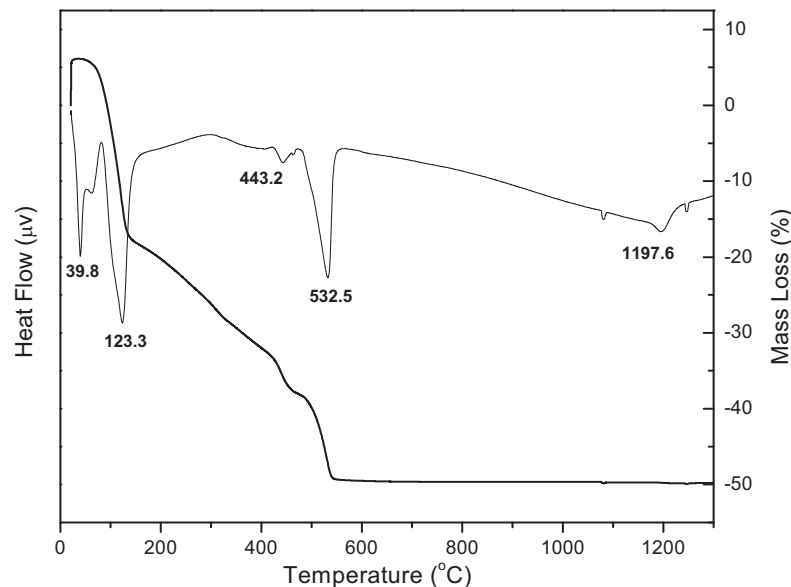

Figure 1. DTA/TG of the as prepared powder

In the TG, the weight loss was complete at about 570°C and three discrete weight-loss regions occurred as seen in the TG diagram. The first region at 44-172°C with 25% weight loss corresponds to the elimination of adsorbed water. This process was indicated as endothermic peak at 38.8°C and shoulder at 60°C in the DTA diagram. The second weight loss region appeared at 172-479°C in the TGA with 18% weight loss which corresponded to elimination of lattice water and was indicated as endothermic peak in the DTA diagram at 443°C. The third weight loss observed in the TG diagram at 479-570°C with a weight loss of 11 % corresponds to the decomposition of the nitrate salts which is also indicated as an endothermic peak at 532°C in the DTA curve.

X-ray diffractometry (XRD) identifying the developed phases, showed following features: a highly crystalline sample gives rise to narrow peaks and a poorly crystalline sample gives rise to broad peaks. "Crystallinity" refers to the degree of structural order in a solid. In a crystal, the atoms or molecules are arranged in a regular, periodic manner. In this respect means the degree of order within the crystal lattice [13]. According to Landi et al., the fraction of crystalline phase (X_C) can be calculated through the equation below [14]:

$$X_C = 1 - \frac{V_{112/300}}{I_{300}}$$

I_{300}: Intensity of peak diffracted from the (300) crystallographic planes of HA.
$V_{112/300}$: Intensity of the valley between the peaks of the planes (112) and (300) of HA.

The average crystallite size was calculated from the broadening in the XRD pattern. According to the Scherrer's equation[15]:

$$L_c = \frac{K\lambda}{\beta Cos\,\theta}$$

L_c: Average crystallite size (nm).
K: Shape coefficient (value between 0.9 and 1.0).
λ: Wavelength of X -ray beam - Cu Kα radiation (λ= 0.15406 nm).
β: Full width at half maximum (FWHM) of HA(211).
Θ: Diffraction angle

The diffraction peak corresponding to the (002) was chosen for calculation of the crystalline size, as it is relatively sharper than the other peaks.
Figure 2 illustrates the XRD patterns of S1 aged gel, dried at 80°C for 48 hours and of the "S6, S8, S12" samples thermally treated at 600, 800, 1200°C for 2 h, respectively. It can be interpreted by the discussion that sharp reflection peak appears in the range of 31.8–40° 2θ for the thermally treated samples "S6, S8, S12", representing the characteristic peak of HA apatite phase (JCPDS09-0432).
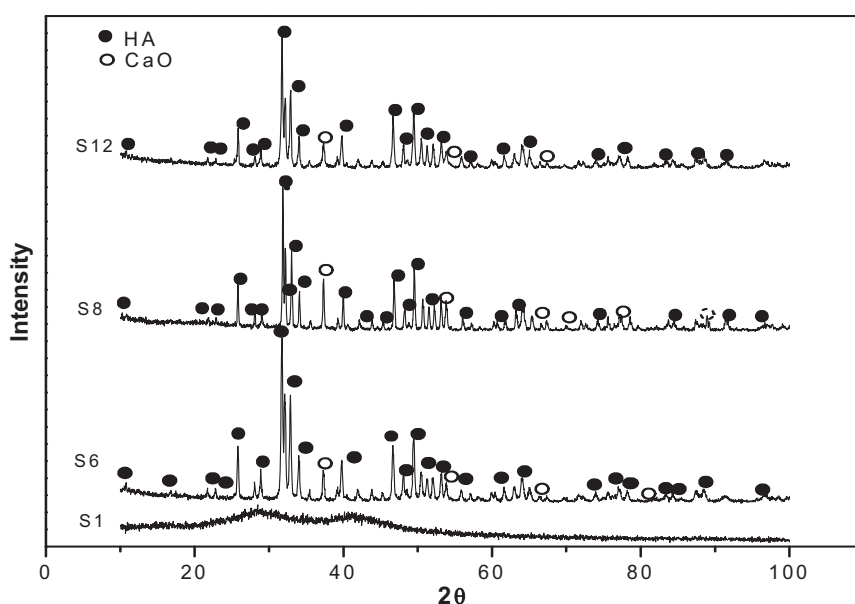

Figure 2. XRD patterns and developed phases of the dried gel (S1) and the powders thermally treated at different temperatures; 600°C (S6), 800°C (S8) and 1200°C (S12).

The XRD pattern of the as-prepared sample S1 is mainly amorphous, and there is no obvious diffraction peak observed. This fact is reported by many authors [16]. As the temperature increases, several peaks appear, which ascribed to the diffraction peaks of the HA phase. The XRD pattern of the S6, S8 and S12 sample thermally treated at 600, 800 and 1200°C respectively, indicates the existence of calcium oxide as traces, together with HA as main phase. The presence of CaO is due to the remaining $Ca(NO_3)_2$ in the precursor system, that can be directly transferred to CaO at high temperature[6]. The degree of crystallinity and calculated crystal size for the thermally treated samples can be seen in Table1. The degree of crystallinity of HA is increased when increasing the temperature from 600 to 800°C (Table 1), but decrease as the temperature increase to 1200°C. The decrease in crystallinity of the 1200°C thermally treated sample (S12) is attributed to the decomposition of HA at corresponding temperature 1200°C, in agreement with the results obtained from the DTA results (Figure 1), while the increase of the crystal size, when compared to 600°C and 800°C thermally treated samples is attributed to an increase of ion migrations when increasing the temperature (Table 1).

Table 1. Crystal size, degree of crystallinity, and electrochemical parameters of the powders thermally treated at different temperatures

Samples	Powders			Coatings		
	Thermal Treatment T(^{o}C)	Degree of Crystallinity (%)	Crystallite Size (nm)	R_i /ohms·cm^2 (after 5 minutes in SBF)	R_f /ohms·cm^2 (after 15 days in SBF)	$\Delta R/R_i$
S6	600	85	40	78610	134550	0.71
S8	800	89	51	5923	1208	-0.8
S12	1200	82	54	-	-	-

Electrochemical impedance spectroscopy (EIS) was used for evaluating the corrosion protection properties of the HA-coatings/Ti6Al4V system. Figure 3 shows the evolution of the electrochemical impedance spectra (Nyquist plots) with the immersion time in SBF for HA-coatings/Ti6Al4V system thermally treated at (A) 600ºC/2h, (B) 800ºC/2h, respectively. Initially, both samples exhibit very similar EIS behaviour. For short immersion time (5 min) the Nyquist plots draw very open arcs with high impedance values. Between 5 min and 1 day of immersion a fast decrease of the impedance values is observed which may be due to the penetration of the SBF through the pores present within the coating as a result of the evaporation of water and ethanol during thermal treatment. However, over time, the evolution of the impedance plots shows a different trend, which depends on the thermal treatment applied for preparing the HA coatings.
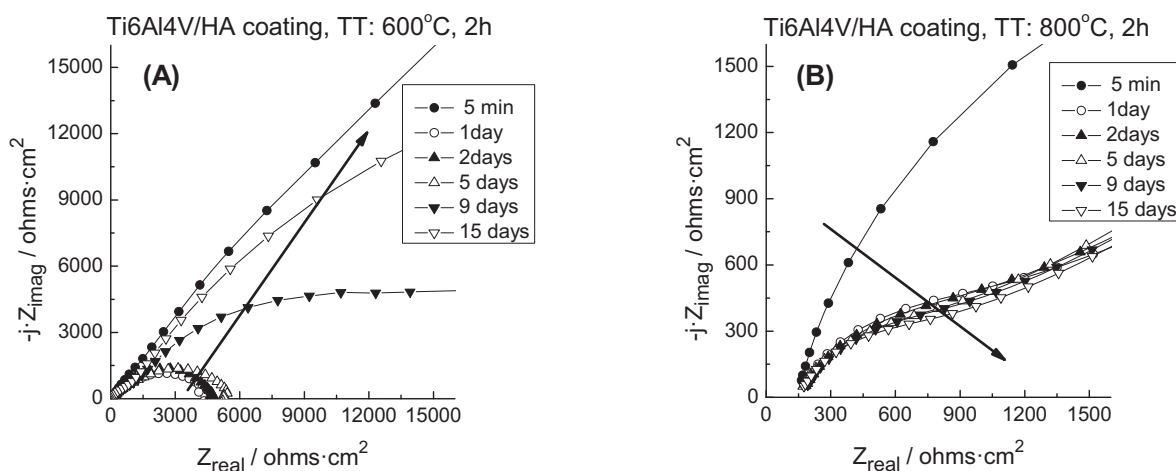

Figure 3 (a, b). Evolution of the electrochemical impedance spectra with the immersion time in SBF for HA-coatings/Ti6Al4V system thermally treated at (A) 600ºC/2h, (B) 800ºC/2h.

The sample thermally treated at 600ºC/2hours exhibits a slow increase of the impedance between 1 day and 5 days. After that, the curvature of the Nyquist arcs are opening quickly and the total impedance reaches comparable values than those observed at the beginning of the immersion tests in the SBF. This behaviour can be due to the blocking of the pores by the formation of precipitates from the solution which prevent further penetrations. For the HA-coatings obtained at 800ºC, the total impedance of the coating decrease continuously upon exposure to the SBF (Figure 3B) and the recovering of the impedance values observed in the samples coated at 600oC is not here evidenced, i.e. 15 days of immersion in the SBF are not enough to block all the pores present in the surface of the HA-coatings obtained at 800ºC.

The evolution of the total resistance of the HA-coatings/Ti6Al4V thermally treated samples during the immersion time in Kokubo's simulated body fluid (SBF) was calculated from the impedance spectra by using the ZView software.

For the determination of the relative variation of total resistance of the metal/coating system, $(\Delta R/R_i)$, the following equation was used:

$$(\Delta R / R_i) = \frac{R_f - R_i}{R_i}$$

where R_i is the initial resistance of the metal/coating system, R_f is the final resistance and, $\Delta R = R_f - R_i$.

Table 1 shows the values of the $(\Delta R/R_i)$ coefficient obtained for thermally treated samples at 600 and 800ºC, respectively. Samples treated at 600ºC showed $(\Delta R/R_i)$ coefficients with positive values (+0.71). This behaviour can be due to the blocking effect of the biomimetic precipitation of HA coming from the SBF which limits the liquid pathways to the metal surface. In contrast, the samples thermally treated at 800ºC show a coefficient with negative values (-0.80) which can be due to the existence of surface cracks which are not able to be blocked by soaking these samples in the SBF.
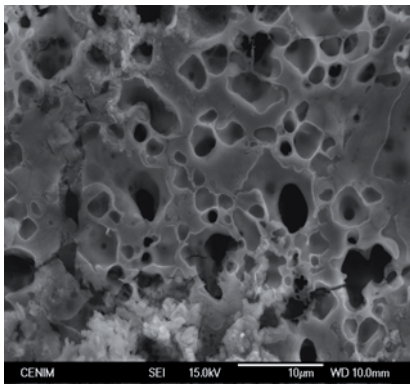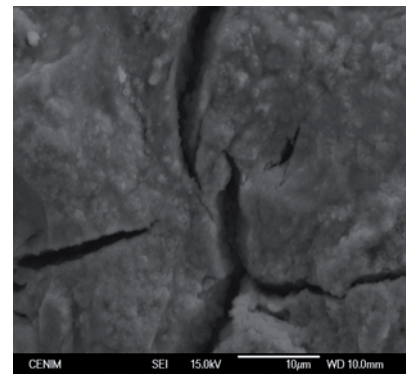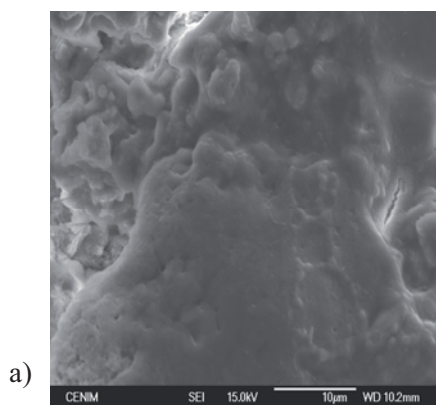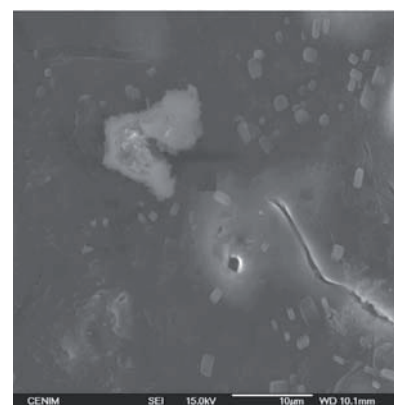

a)   b)

Figure 4 (a, b). SEM micrographs obtained for the HA-coatings/Ti6Al4V system thermally treated at (a) 600°C/2h, (b) 800°C/2h before immersion in SBF.

The SEM micrographs obtained for the surface of the HA coatings before immersion in SBF are shown in Figure 4 (A, B). The surface of the sample thermally treated at 600ºC (Figure 4A) shows the presence of pores due to the evaporation of both, water and ethanol during thermal treatment. While the surface of the sample thermally treated at 800ºC (Figure 4B) show the presence of extensive cracks probably due to a thermal expansion coefficient mismatch between the coating and the substrates during cooling[17].

a)   b)

Figure 5. SEM micrographs obtained for the HA-coatings/Ti6Al4V system thermally treated at (a) 600°C/2h, (b) 800°C/2h after immersion in a SBF solution.

After 15 days of immersion in SBF the surface of both samples is covered with a bone-like apatite layer which proved that both samples are bioactive. The surface of the sample thermally treated at 600ºC is completely covered with these precipitations from SBF (Figure 5A), while the surface of the sample thermally treated at 800ºC is not completely covered (Figure 5B), as still some cracks are observed by SEM at the surface. These results are in agreement with those obtained by EIS.

5. Conclusions

- The crystallite size and degree of crystallinity of the HA sol-gel powders, which are precursors of the hydroxyapatite nano-crystalline coatings, strongly depends on the thermal treatment applied.
- Based on this knowledge, hydroxyapatite nano-crystalline coatings on Ti6Al4V alloy can be obtained by sol-gel route.
- Among all the coatings prepared, the HA coating/Ti6Al4V system obtained by thermal treatment at 600ºC for 2 hours shows the best barrier properties against the *in vitro* corrosion of the metal substrate.
- All the prepared samples exhibit good bioactivity upon immersion in SBF at 37.5ºC for 15 days. Among all of them, the 600ºC thermally treated sample shows the best behaviour in terms of *in vitro* bioactivity.

Acknowledgements

References

[1]   M. Vallet-Regi, J.M. Gonzalez-Calbet, *Prog. Solid State Chem.*, **32**, 1(2004).
[2]   L.L. Hench*, J. Am. Ceram. Soc.*, **81**, 1705 (1998).
[3]   A. Slosarczyk, E. Stobierska, Z. Paszkiewicz, M. Gawlick, *J. Am. Ceram. Soc.*, **79**, 2539 (1996).
[4]   M. Yoshimura, H. Suda, K. Okamoto, K. Ioku, *J. Mater. Sci.*, **29**, 3399 (1994).
[5]   D.M. Liu, T. Troczynski, W.J.J Tseng, *Biomaterials*, **22**, 1721(2001).
[6]   M.F. Hsieh, L.H. Perng, T.S. Chin, H.G Perng, *Biomaterials,* **22**, 2601(2001).
[7]   E. Peon, A. Jimenez-Morales, E. Fernandez-Escalante, M.C. Garcia-Alonso, M.L. Escudero, J.C. Galván, *Rev. Metal. Madrid*, Sp. Iss. 479 (2005).
[8]   K. DeGroot, C.P.A.T. Klein, J.G.C. Wolke, J.M.A. De Blieck-Hogervorst, in "*CRC Handbook of Bioactive Calcium Phosphates*", edited by T. Yamamuro, L.L. Hench and J. Wilson, p. 3 (CRC Press, Boca Raton, FL, 1990).
[9]   Diangang Wang, Chuanzhong Chen, Ting He, Tingquan Lei, *J. Mater. Sci.: Mater. Med.*, **19**, 2281(2008)
[10]   Seok Kim, Prashant N. Kumta, *Mater. Sci. Eng. B.*, **111,** 232 (2004).
[11]   D.G.Wang, C.Z. Chen, J. Ma, G. Zhang, *Colloid Surf. B-Biointerfaces*, **66**, 155 (2008).
[12]   Kui Cheng, SAM Zhang, W.J. Weng, *J. Sol-Gel Sci. Technol.*, **38**, 13 (2006).
[13]   M. Epple, *Z Kardiol*. 2001;90 Suppl 3:64-7.
[14]   E. Landi, A. Tampieri, G. Celotti, S. Sprio, *J. Eur. Ceram. Soc.*, **20**, 2377 (2000).
[15]   H.P. Klung, E. Alexander, "*X-Ray Diffraction Procedures: For Polycrystalline and Amorphous Materials*", 2nd Edition New York: John Wiley; (1974).
[16]   Yanbao Li, Dongxu Li, *J. Appl. Ceram. Technol.*, **5**, 442 (2008).
[17]   M.Wei, A.J.Ruys, B.K. Milthorpe, C.C. Sorrell, J.H. Evans. *J. Sol-Gel Sci. Technol* **21,** 39–48, (2001).